

NEW APPLIED METHOD FOR SIMULTANEOUS DETERMINATION OF ELLAGIC AND TANNIC ACID BY MULTI-WALL CARBON NANOTUBE PASTE ELECTRODE: APPLICATION IN QUANTIFICATION *PUNICA GRANATUM* AND *QUERCUS INFECTORIA*

S. M. GHOREISHI*, M. BEHPOUR, M. KHAYATKASHANI,
M. H. MOTAGHEDIFARD

Department of Analytical Chemistry, Faculty of Chemistry, University of Kashan, Kashan, I.R. Iran

We investigated the electrochemical properties of ellagic acid (EA) and tannic acid (TA) by using a bare and modified carbon paste electrode containing multi-wall carbon nanotubes (MWCNTs). Voltammetric methods including cyclic voltammetry, chronocoulometry, linear sweep voltammetry, anodic stripping differential pulse voltammetry and hydrodynamic voltammetry were used. Cyclic voltammetry was used to investigate the redox properties of the modified electrode at various scan rates. Electrochemical parameters including the diffusion coefficient (D), the electron transfer coefficient (α), the ionic exchanging current density (i_0) and the redox reaction rate constant (k) were determined for the oxidation of EA and TA on the surface of our modified electrodes. High dynamic ranges and low detection limits were obtained for both compounds. The peak current increased linearly with the concentration of EA and TA. The detection limits for EA and TA in the anodic stripping differential pulse voltammetry experiments were estimated to be 2.1×10^{-10} and 6.7×10^{-10} M, respectively, over the 180 second accumulation times of the open circuit potential. The modified electrode was then successfully used to determine the concentration of EA and TA in *punica granatum* and in the galls of *Quercus infectoria*.

(Received September 20, 2010; accepted March 14, 2011)

Keywords: Ellagic acid; Tannic acid; Punica granatum; Quercus infectoria; Multi-wall carbon nanotubes; Voltammetry.

1. Introduction

Tannins are plant secondary metabolites that are known to exist in hydrolyzable and condensed forms. Most dietary tannins are water hydrolyzable and are predominantly composed of gallotannin or ellagitannin. TA, a gallotannin, has a structure that consists of multiple gallic acid esters of glucose. TA is considered to be a safe food additive when present in the range of 10 to 400 ppm. The exact safe limit depends upon the type of food in which it is present.

*Corresponding author: s.m.ghoreishi@kashanu.ac.ir

TA is known for its anti-mutagenic, anticancer and antioxidant properties [1]. Recent studies have revealed that its antioxidant activity may be correlated with its copper chelating ability [2]. Its abilities to reduce serum cholesterol and triglycerides as well as to suppress insulin lipogenesis are also well-documented [3, 4]. TA anti-microbial properties are associated with the ester linkage between the gallic acid substituent and other sugar or alcohol groups. TA is often used as an additive in medicinal products including those used for treatment of burns and diarrhea. Therefore, determination of the concentrations of TA is of importance for food, medical and industrial goods production [5-7]. TA naturally occurs in the bark and fruits of many plants [8]. In living organisms, it chelates iron through the use of its ten galloyl groups, and it diminishes intestinal non-heme iron absorption [9, 10].

EA (Scheme 1) is a polyphenol dimeric derivative of gallic acid with high antioxidant activity. The main sources of EA and ellagitannins are oak trees (*Quercus robur*, *Quercus alba*), walnut trees (*Juglans nigra*) and chestnut trees (*Castanea sativa*). Berry fruits are also a source of ellagitannins and EA. These include strawberries, raspberries, and blackberries. Other sources include seeds and nuts, including pecans and regular fruits such as pomegranate. *Punica granatum* and *Quercus infectoria* have been reported to contain high concentration of tannins in both the hydrolyzable and condensed forms.

Development of new methods for simultaneous determination of EA and TA has received considerable interests in recent years. Various methods such as chromatography [11], spectrophotometry [12] and capillary electrophoresis (CE) [13] have been developed for this purpose. These techniques are limited by poor accuracy or the need for expensive instrumentation with high operating costs. Among the various methods reported for EA and TA determination, electrochemical techniques are often preferred because of their high selectivity, rapid detection, low cost and their lack of a substantial sample preparation setup. Electrochemical methods that use chemically modified electrodes have been widely used as sensitive and selective analytical tools for environmental, clinical and biotechnical analyses [14, 15]. Recently, an electrochemical sensor has been developed for the evaluation of TA concentration [16, 17]. However, to our knowledge, no work has been reported on carbon nanotube- modified carbon paste electrode use to study the oxidation of EA and TA. In this study, we report a novel sensor for the simultaneous determination of EA and TA in *Punica granatum* and *Quercus infectoria* by electrochemical methods based on a carbon paste electrodes that are modified with multi-wall carbon nanotubes.

2. Experimental

2.1. Reagents

EA and TA were purchased from Sigma and used without any further purification. Pure fine graphite powder (Merck) and paraffin oil (DC = 350, Merck, $\rho = 0.88 \text{ g cm}^{-3}$) were used as binding agents for the graphite pastes. Multi-wall carbon nanotubes (MWCNTs) were obtained from the Chinese Academy of Sciences and had outside diameters of 10-20 nm, lengths of less than 1-2 μm and purities of over 95%. EA and TA solutions were prepared immediately prior to use, and all experiments were carried out at ambient laboratory temperatures (25 °C). Briton–Robinson buffer solutions (B-R solutions, 0.2 M) of different pH values were prepared from stock solutions of 0.2 M H_3PO_4 , CH_3COOH , H_3BO_3 and NaOH . All solutions were freshly prepared using double distilled water. Herbal extracts were purchased from the traditional medicine department of the Barij Essence Pharmaceutical Company (Kashan, Iran).

2.2. Apparatus

All electrochemical experiments were carried out using an Autolab potentiostat-galvanostat PGSTAT 35 (Eco chemie Utrecht, Netherlands) equipped with GPES 4.9 software. The electrochemical cell was equipped with a modified carbon paste disk as the working electrode, a platinum electrode as the counter electrode, and a silver/silver chloride (Ag/AgCl) electrode as

the reference electrode. A personal computer (pentium IV) was used for data storage and processing. The body of the carbon paste-based working electrode consisted of a Teflon syringe with a rod (2 mm diameter and 5 mm depth) bored at one end that was filled with paste. A copper wire was placed through the center of the rod to contact the paste. The working electrode was pretreated by pushing paste out of the tube, removing the excess, and mechanically polishing the surface on a piece of weighing paper. A digital pH meter (Metrohm model 691) was used when preparing buffer solutions. These buffer solutions served as the supporting electrolyte in the voltammetric experiments. The rotating electrode system, an AFMSRX 1270 rotator, from Pine Instrument Company (Grove City, PA, USA) and an MSRX speed controller were used. An ultrasound bath (Bandelin Sonorex, Germany) was used at a constant frequency of 35 kHz during experimentation.

2.3. Preparation of carbon paste electrodes (CPEs)

The bare carbon paste electrode (CPE) was prepared by thoroughly mixing 80.0% (w/w) graphite powder and 20.0% (w/w) paraffin oil. The carbon paste electrode that was modified with multi-wall carbon nanotubes (MWCNT/CPE) was prepared by mixing 78.0% (w/w) graphite powder with 2.0% (w/w) carbon nanotubes. The carbon nano tubes were dispersed in the water by an ultrasound bath for 30 minutes. After the vaporization of water, a 20.0% (w/w) of paraffin oil was added to the mixture. A portion of the resulting paste was packed into the cavity (2 mm i.d. and 10 cm length) of a polytetrafluoroethylene (PTFE) tube. Electrical contacts to the paste were established by inserting a copper wire into the syringe, through to the back of mixture. The surface was smoothed on a piece of weighing paper. New paste surfaces were obtained by pushing an amount of paste out of the tube, removing the excess paste, and polishing the newly formed electrode surface. A modified carbon paste disk served as the working electrode for RDE experiments. The body of the carbon paste-based working electrode consisted of a Teflon rod with a hole (2 mm diameter and 10 mm depth) bored into one end, into which the filling was placed. Contact to the paste was made with a stainless steel wire that was inserted through the center of the rod and then screwed onto the RDE device. Results showed that 2.0% (w/w) was the optimal amount of CNTs to add. The peak current of the CNT/CPE (i.e., the highest CNT/CPE of all of the investigated electrodes) was approximately two times and one and one half times greater than for bare CPEs in the cases of TA and EA measurements, respectively. The peak current increased rapidly with increases in accumulation time, but it became relatively stable at 150 s. This indicates that EA and TA accumulated on the CNT/CPEs. However, an accumulation time of 150 s was achieved with an open circuit as well.

2.4. Sample preparation

To prepare herbal extracts, 1.0 g of dried powder was weighed and added to 10 ml of doubly distilled water:ethanol (30:70) at 50 °C. Samples were protected from light, immersed in an ultrasound bath and subjected to ultrasound treatment at a constant frequency of 35 kHz for 30 min at room temperature. The ethanolic extracts were filtered through Whatmann No.1 filter paper. The extracts were concentrated under reduced pressure at a temperature of 45 °C and then freeze dried.

3. Results and discussion

3.1. Influence of pH on the bulk-modified electrode

The electrochemical responses of EA and TA molecules are generally pH dependent. Thus, the electrochemical behavior of TA on the surface of MWCNT/CPE was studied at different pH values of 0.2 M B-R buffer solutions using anodic stripping differential pulse voltammetry (Fig. 1). Anodic peak potentials of the EA and TA were shifted to less positive values with

increasing pH. The maximum anodic currents for EA and TA (Fig. 1A) were obtained at a pH of 2.0 using 0.2 M B-R buffers. Thus, solutions of pH 2.0 were used in all subsequent experiments. In the Nernst equation (Eq. 1), n and m represent the number of electrons and protons involved in reaction, respectively, and a and b represent the stoichiometric coefficients of the reagents in reaction equation. The slopes of -68.5 and -69.8 mV pH^{-1} for EA and TA, respectively, (Fig. 1B) that were derived from the Nernst equation indicate that the ratio of the electrons to protons in the reaction is 1:1. From the intercept of the curves shown in inset B of Fig. 1, the standard formal potentials (E°) of EA and TA were found to be 855.8 and 686.9 mV, respectively.

$$\text{Eq. 1: } E_p = E^\circ + (0.0591/n) \log [(Ox)^a/(R)^b] - (0.0591 m/n) \text{pH}$$

$$\text{For EA: } E_{pa} \text{ (V vs. Ag/AgCl)} = 0.8558 - 0.068 [\text{pH}]$$

$$\text{For TA: } E_{pa} \text{ (V vs. Ag/AgCl)} = 0.6869 - 0.069 [\text{pH}]$$

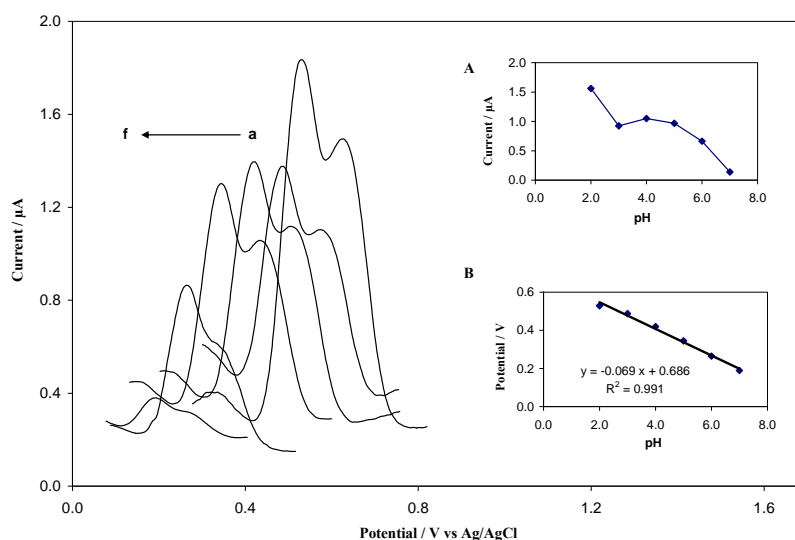


Fig. 1 Anodic stripping differential pulse voltammograms of a 12 nM TA solution corresponding to pH values of 2, 3, 4, 5, 6 and 7 with a constant scan rate 25 mVs^{-1} . Insets: (A) Plot of intensity I/A versus pH and (B) a plot of electrochemical potential E_{pa}/V versus pH.

3.2. Chronocoulometry measurements

The anodic oxidations of EA and TA by MWCNT/CPEs were studied by chronocoulometry. Chronocoulograms of EA and TA solutions in the concentration range of 7.5 to $60.0 \mu\text{M}$ and 15.0 to $60.0 \mu\text{M}$ (Fig. 2), respectively, were taken using a potential step of 1.0 V. From these chronocoulometric studies, the diffusion coefficients of EA and TA in the modified electrodes can be determined. For electroactive materials such as EA and TA with diffusion coefficients of D , the current for the electrochemical reaction (at a mass transport limited rate) is described by the Cottrell equation [18]:

$$\text{Eq. 2 } Q = 2nFAD^{1/2} C \pi^{-1/2} t^{1/2}$$

where D ($\text{cm}^2 \text{ s}^{-1}$) and C (mol cm^{-3}) are the diffusion coefficient and the bulk concentration, respectively. Under diffusion limited transport (mass transport), a plot of Q versus $t^{1/2}$ should be linear, and the value of D can be extracted from the slope. Inset B of Fig. 2 shows the fitted experimental plots for different concentrations of TA. The slopes of the resulting straight lines were plotted versus the EA or TA concentrations. According to the integrated Cottrell equation,

the diffusion coefficients for EA and TA were determined using an electrochemical approach and were found to be 6.49×10^{-7} and 1.89×10^{-6} $\text{cm}^2 \text{s}^{-1}$, respectively.

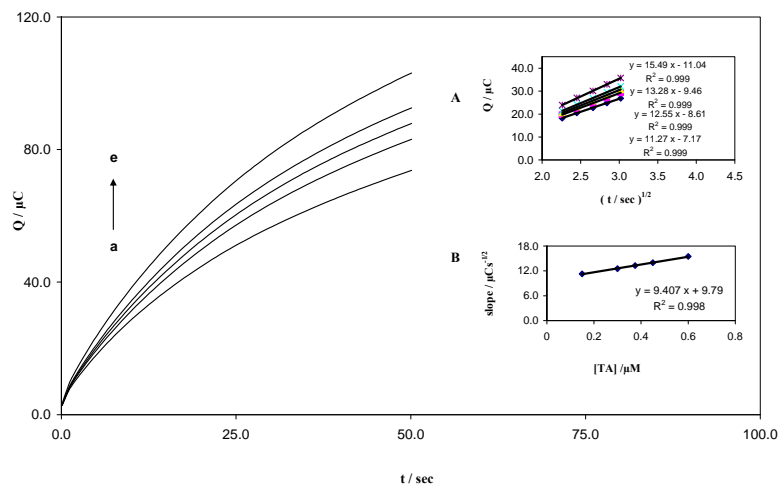


Fig. 2 Chronocoulograms obtained from MWCNT/CPE in a 0.2 M B-R buffer solution (pH = 2.0) with varying concentrations of TA. Curves a - e correspond to TA concentrations of 15, 30, 37, 45 and 60 μM , respectively. Insets: (A) Plots of Q versus $t^{1/2}$ obtained from chronocoulograms a-e, and (B) the slope of the straight lines versus TA concentration.

3.3. Linear sweep voltammetry measurement of the oxidation of EA and TA

Fig. 3 shows the linear sweep voltammograms of a MWCNT/CPE obtained in a 0.2 M B-R buffer solution (pH 2.0) containing different concentrations of TA. The sweep rate was 25 mV s^{-1} . The points in this figure show the rising part of the voltammogram (known as the Tafel region), which is affected by the electron transfer kinetics between the analyte and the modified electrode. If deprotonation of TA is sufficiently fast, then the number of electrons involved in the rate determining step can be estimated from the slope of the Tafel plot. Inset A of Figure 3 shows the Tafel plots that were derived from the points of the Tafel regions of the linear sweep voltammograms. The average Tafel slopes of $0.0879 \text{ mV decade}^{-1}$ that were obtained in this experiment agree with hypothesis that one electron is involved in the rate determining step of the electrode process. This assumes a charge transfer coefficient of $\alpha = 0.26$. Further, the ionic exchanging current density (i_0) was found by averaging the Tafel intercepts and determined for TA to be $1.6 \mu\text{A cm}^{-2}$.

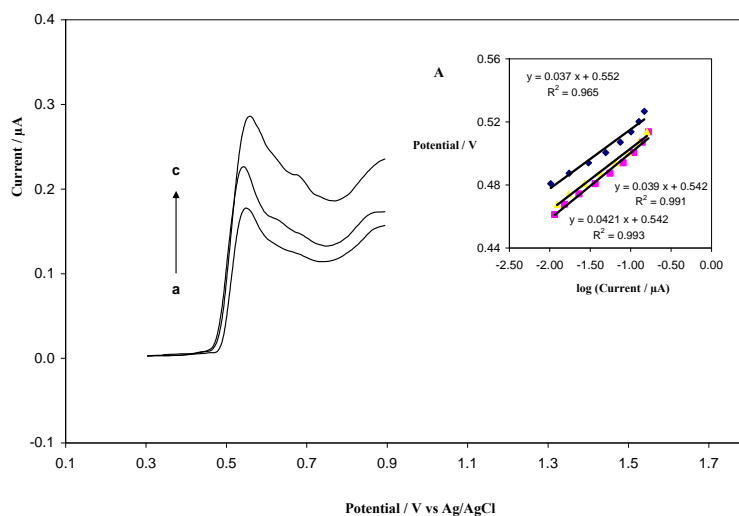


Fig. 3 Linear sweep voltammograms of MWCNT/CPE in B-R buffer (pH = 2.0) containing 4, 5 and 6 μM TA (a-c, respectively). Inset A: Tafel plot derived from linear sweep

voltammograms.

According to the average Tafel slopes for EA, it appears that two electrons were involved in the rate determining step of the electrode process. This assumes a charge transfer coefficient of $\alpha = 0.33$ and that the ionic exchanging current density gathered by averaging the Tafel intercepts was $1.7 \mu\text{A cm}^{-2}$.

3.4. Cyclic voltammetric studies of EA and TA at MWCNT/CPEs

The effect of the scan rate on the oxidation of EA and TA at the MWCNT/CPEs was investigated by cyclic voltammetry. As can be observed in Fig. 4, the oxidation peak potential shifted with increasing scan rates toward a more positive potential, confirming that there was a kinetic limitation of the electrochemical reaction. Plots of the peak heights (I_p s) versus the square root of scan rates ($v^{1/2}$) in the range of 25-105 mV and 25-75 mV for EA and TA (Fig. 4A), respectively, were constructed. These plots were found to be linear, suggesting that, the processes were diffusion-controlled rather than surface-controlled. From these plots, an approximate total number of electrons, n , in the overall oxidation of EA and TA were calculated using the following equation for diffusion-controlled electrochemically irreversible reactions in which the first electron transfer is rate-determining [18]:

$$\text{Eq. 3: } I_p = 2.99 \times 10^5 n [(1-\alpha) n_a]^{1/2} AC^*D^{1/2}v^{1/2}$$

where D is the diffusion coefficient of EA and TA (6.49×10^{-7} and $1.89 \times 10^{-6} \text{ cm}^2 \text{ s}^{-1}$ respectively) as obtained by chronocoulometry, C^* is the bulk concentration of EA and TA (33.0 and $7.3 \mu\text{M}$, respectively) and A is the electrode surface area (0.0314 cm^2). Values for α and n_a were derived from the Tafel plots and yielded values of 0.33 and 1 for EA and 0.26 and 2 for TA, respectively. To obtain information about the rate-determining step, the Tafel plot was determined by the linear sweep voltammetry method. This produced an approximate value for the total number of electrons involved in the anodic oxidation of EA and TA of $n = 2.28$ and 1.90 , respectively.

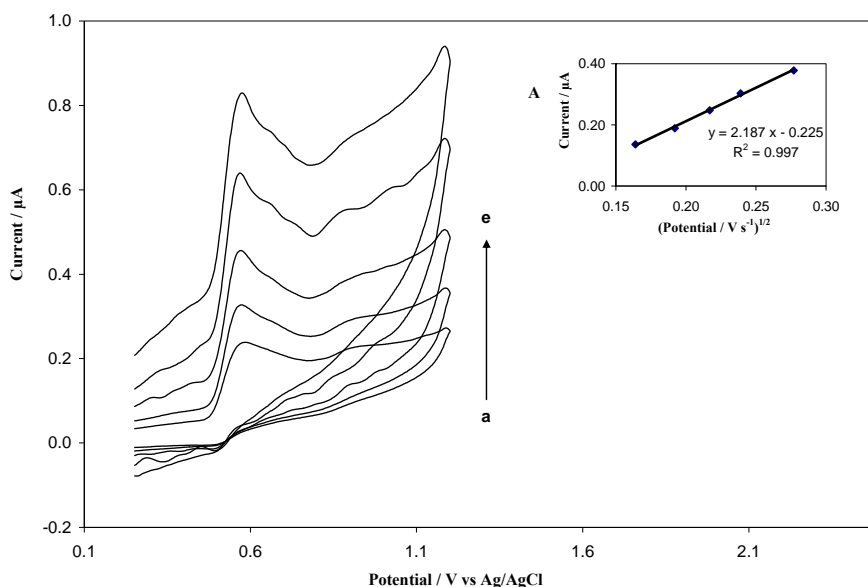


Fig. 4 Cyclic voltammetry of MWCNT/CPE for a TA concentration of $70 \mu\text{M}$ at scan rates of $25\text{-}75 \text{ mV s}^{-1}$ (from inner to outer plots). Inset (A): Plot of peak current versus E/mV .

3.5. Rotating disk electrode (RDE) voltammetry

In this paper, we report the first use of RDE voltammetry and a carbon paste electrode to examine the electrocatalytic activity of MWCNT/CPEs in the oxidation of EA and TA. Steady-state I-E curves were recorded for the oxidation of EA and TA on MWCNT/CPEs under various experimental conditions. A typical example of the I-E curves (RDE voltammograms) at rotation speeds ranging from 500-4500 rpm is shown in Fig. 5 for a 0.02 mM solution of TA. In this case, when the oxidations of EA and TA at the surface of the MWCNT/CPEs are controlled solely by mass transfer in the solution, the relationship between the limiting current and rotating speed should obey the Levich equation [18]:

$$\text{Eq. 4: } I_1 = I_{\text{Lev}} = 0.62 nFAD^{2/3} \nu^{-1/6} \omega^{1/2} C$$

where D ($\text{cm}^2 \text{s}^{-1}$), ν ($\text{cm}^2 \text{s}^{-1}$), ω (rad s^{-1}) and C (mol cm^{-3}) are the diffusion coefficient, the kinematics viscosity, the rotation speed and the bulk concentration of the reactant in the solution, respectively. All other parameters have their conventional meanings. Based on Equation 4, the plot of the limiting current I_1 as a function of $\omega^{1/2}$ (rad s^{-1})^{1/2} should be a straight line. According to the Levich plot (inset A of Fig. 5), the current increases with increasing electrode rotation speed, but the trends were found to be nonlinear due to kinetic limitations. For an irreversible reaction, the relationship between the limiting current and the rotating speed is given by the Koutecky-Levich equation [18]:

$$\text{Eq. 5: } \Gamma^{-1} = (nFAkCT)^{-1} + (0.62 nFAD^{2/3} \nu^{-1/6} \omega^{1/2} C)^{-1}$$

where A (cm^2), C (mol cm^{-3}), k ($\text{cm}^3 \text{mol}^{-1} \text{s}^{-1}$), Γ (mol cm^{-2}), D ($\text{cm}^2 \text{s}^{-1}$), ν ($\text{cm}^2 \text{s}^{-1}$) and ω (rad s^{-1}) are the electrode area, substrate concentration, catalytic rate constant, surface coverage, diffusion coefficient, kinematics viscosity and rotation speed, respectively. It can be seen that the intercept of the linear plot is positive, clearly indicating that there is a kinetic limitation of the electrode process. In addition, the slope and intercept are inversely proportional to the bulk concentration of either EA or TA, suggesting that the current is not limited by the rate of electron transport within the electrode.

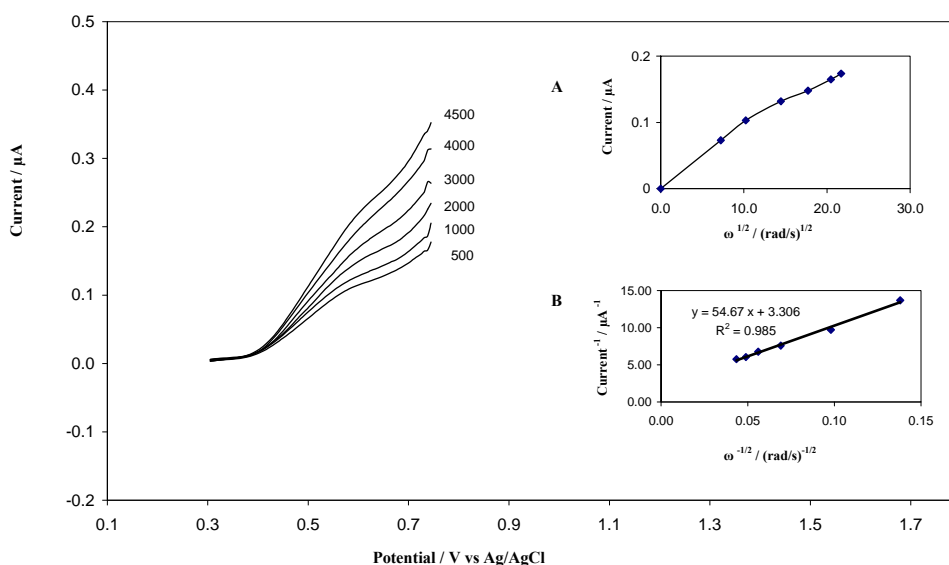


Fig. 5 Typical steady-state voltammograms obtained for the MWCNT/CPEs in B-R buffers ($\text{pH} = 2.0$) containing 0.02 mM TA at various rotation rates. Insets: (A) Levich plot for TA

oxidation on the CNT/CPEs, and (B) the Koutecky–Levich plot obtained from data derived from the Levich plot.

According to Equation 6, the plot of I^{-1} versus $\omega^{-1/2}$ gives a straight line (as shown in inset B of Fig. 5). The rate-determining step must be found in the catalytic process at the electrode surface or in the electron diffusion process within the electrode. The value of the rate constant ($k/\text{cm}^3 \text{ mol}^{-1} \text{ s}^{-1}$) for the catalytic reaction can be obtained from the intercept of the Koutecky–Levich plot. The values of the rate constant for the MWCNT/CPEs were found to be 1.2×10^{-2} and $2.5 \times 10^{-3} \text{ cm}^3 \text{ mol}^{-1} \text{ s}^{-1}$ for EA and TA at a concentration of 0.02 mM, respectively. When one determines the diffusion coefficients with an RDE, it is common to change the rotation rate (ω in rad sec^{-1}) and plot I_1 versus $\omega^{1/2}$. The slope of the resulting best-fit line can be used to determine D:

$$\text{Eq. 6:} \quad D = (\text{slope}_{\text{Lev}} / 0.62 n \text{ FAC } \nu^{-1/6})^{3/2}$$

As with chronoamperometry, there are limits to the range of experimental conditions under which Equation 6 applies, but with the RDE, the important parameter is the rotation rate, ω . If, in RDE experiments, ω has been applied in the range of 10–10000 rpm, the diffusion coefficient of EA or TA may be obtained from the slope of the Levich plot [19]. So, the mean values of D in $\text{cm}^2 \text{ s}^{-1}$ for EA and TA were found to be 6.80×10^{-7} and $1.27 \times 10^{-6} \text{ cm}^2 \text{ s}^{-1}$, respectively.

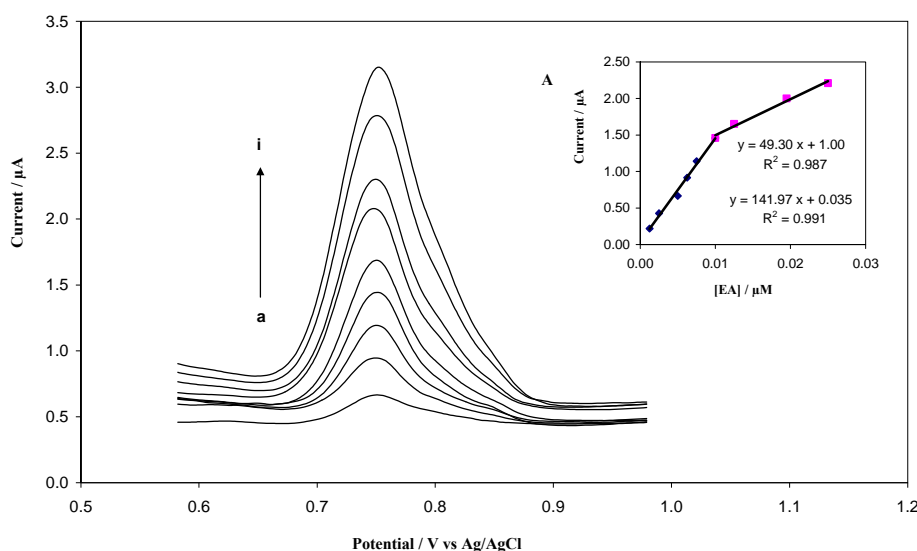


Fig. 6 Anodic stripping differential pulse voltammograms of MWCNT/CPE in 0.2 M B-R buffer solutions (pH = 2.0) containing different concentrations of EA. Curves a-i correspond to EA concentrations of 1.25–25 nM. Inset A: Plots of the peak current as a function of EA concentration in the ranges of 1.25 to 10 nM and 10 to 25 nM.

3.6. Calibration plots and the limits of detection for EA and TA at the MWCNT/CPE

Because anodic stripping differential pulse voltammetry (ASDPV) has a much higher current sensitivity and better resolution than cyclic voltammetry, it was used to estimate the detection limits for EA and TA. In addition, the charging current contribution to the background current, which is a limiting factor in the analytical determinations made with cyclic voltammetry, is negligible in ASDPV mode. Fig. 6 and 7 show the ASDPV data obtained for the oxidation of different concentrations of EA and TA on the MWCNT/CPEs in 0.2 M B-R buffer solutions (pH = 2.0) at a scan rate of 25 mV s^{-1} . The dependencies of the peak currents on the EA and TA

concentrations are shown in inset A of Fig. 6 and 7, respectively. These figures clearly show that the plot of peak current versus EA concentration is composed of two linear segments with different slopes. These line segments correspond to two different ranges of substrate concentrations. The decrease in sensitivity (slope) of the second linear range is likely due to the kinetic limitation. From the analysis of these data, we estimate that the detection limits of EA and TA (with a signal to noise ratio of greater than 3) is of the order of 2.1×10^{-10} and 6.7×10^{-10} M, respectively. The relative standard deviation (RSD) of 3.17% in the oxidation peak current and 0.82% in the peak potential for five repeated detections of 7.5 nM EA suggests that there is excellent reproducibility of results using our modified electrode.

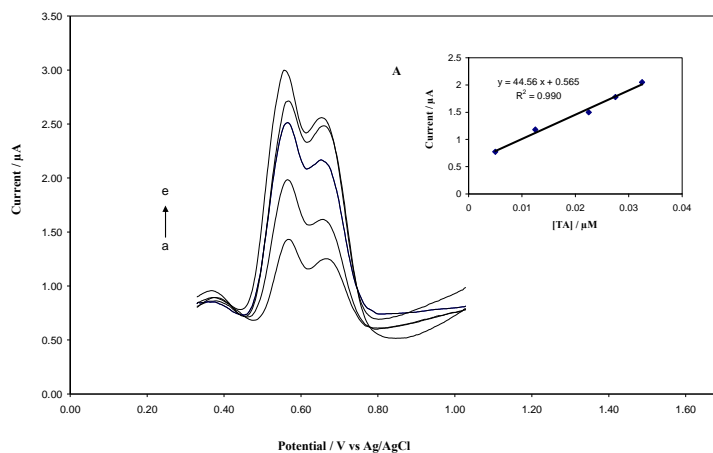


Fig. 7 Anodic stripping differential pulse voltammograms of MWCNT/CPE in 0.2 M B-R buffer solutions (pH = 2.0) containing different concentrations of TA. Curves a-e correspond to TA concentrations of 5-32.5 μ M. Inset A: Plots of the peak current as a function of TA concentration in the range of 5-32.5 μ M.

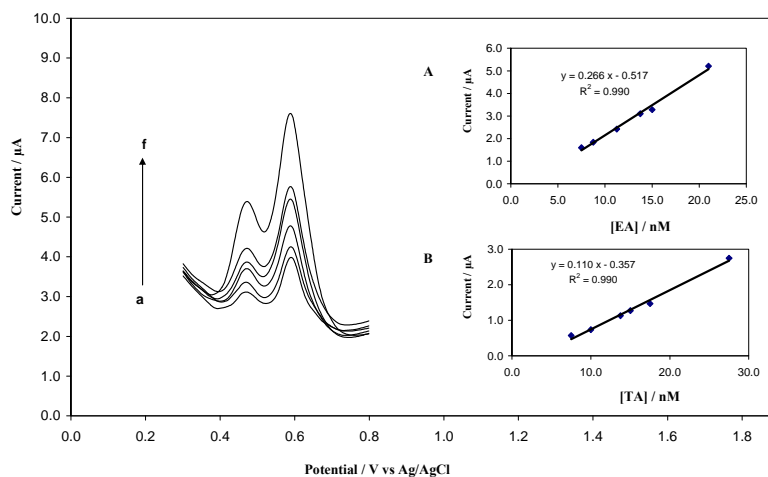


Fig. 8 Anodic stripping differential pulse voltammograms of MWCNT/CPE in 0.2 M B-R buffer solutions (pH = 2.0) containing different concentrations of EA and TA. Insets: (A) Plot of peak current as a function of EA concentration in the linear range of 7.5-21 nM EA, and (B) a plot of peak current as a function of TA concentration in the linear range of 7.5-27.5 nM TA.

3.7. Simultaneous determination of EA and TA at the surface of MWCNT/CPE

One of the main objectives of this study was to develop and test a modified electrode that was capable of measuring the oxidation of EA and TA separately from the detection of their electrochemical responses. ASDPV was used to estimate EA and TA concentration simultaneously. In the first stage, according to the curves of E versus pH for EA and TA, the optimum pH for the maximum response of both drugs was found to be 2.0. The peak currents for EA and TA increased linearly with their respective concentrations within specific ranges of concentrations. The calibration parameters used for the simultaneous determination of EA and TA concentration are shown in Fig. 8. The sensitivity of the modified electrode toward the oxidation of EA was found to be $0.266 \mu\text{A } \mu\text{M}^{-1}$, whereas the sensitivity toward EA in the absence of TA was found to be $0.110 \mu\text{A } \mu\text{M}^{-1}$. It is interesting to note that the sensitivities of the modified electrodes towards EA and TA when alone or mixed are very similar. This indicates that the oxidation processes of EA and TA at the MWCNT/CPE are independent. These results also indicate that either the simultaneous or independent measurement of these two analytes is possible without the occurrence of any interference. If the EA or TA signals were affected by the presence of another analyte, the above-mentioned slopes would be different.

3.8. Determination of EA and TA in *Punica granatum* and *Quercus infectoria*

To our knowledge, the determination of EA and TA in the peels of *Punica granatum* and the gall of *Quercus infectoria* by ASDPV has not been reported. In this paper, we report the novel use of MWCNT/CPEs to detect the oxidation of EA and TA by ASDPV, and we compare our method with HPLC methods to examine herbal extracts. Determination of EA and TA in *Punica granatum* peels and *Quercus infectoria* extracts was achieved by the standard addition method. A linear equation ($i_p (\mu\text{A}) = 0.353 C (\text{nM}) + 1.168$) was obtained with a correlation coefficient of 0.996 for *Quercus infectoria* gall extract using this method. The quantity of TA in 1 g of gall obtained using ASDPV was found to be $178.0 \pm 5.0 \text{ mg g}^{-1}$ (Table 1), which is in agreement with results obtained by HPLC [20]. Recovery experiments were conducted to evaluate the matrix effects. We determined that satisfactory recoveries from the extracts of 98.5% were obtained. Thus, matrix interferences were not significant in the samples analyzed by ASDPV. Simultaneous determination of EA and TA in *Punica granatum* peel extracts was achieved by the standard addition method, where the following linear fits were obtained:

$$\begin{aligned} \text{For TA:} \quad & i_p (\mu\text{A}) = 0.232 C (\text{nM}) + 0.100, R^2 = 0.996 \\ \text{For EA:} \quad & i_p (\mu\text{A}) = 0.378 C (\text{nM}) + 0.203, R^2 = 0.993 \end{aligned}$$

Table 1. EA and TA in one gram of herbal extract

Sample	herbal extract	ellagic acid (mg g^{-1})	tannic acid (mg g^{-1})
1	<i>punica granatum</i>	5.6 ± 0.5	2.1 ± 0.2
2	<i>quercus infectoria</i>	-----	178.0 ± 2.0

The average recovery percentages of TA and EA were 98.7% and 105.4% for *Punica granatum*, respectively. According to these results, the TA content and EA content in these extracts were 2.1 ± 0.2 and $5.6 \pm 0.5 \text{ mg g}^{-1}$, respectively (Table 1). These results concur with those measured by HPLC [21].

4. Conclusions

This work describes a novel and selective method for the simultaneous determination of EA and TA. An increase in the current response and a decrease in the anodic overpotential are observed relative to the electrochemical response of a bare CPE. High sensitivity, low detection limits, easy regeneration of the electrode surface, low cost, simple preparation, excellent stability and good reproducibility make the MWCNT/CPE system very useful for the determination of EA and TA in *Punica granatum* peel and *Quercus infectoria* gall extracts.

Acknowledgments

The authors would like to thank the University of Kashan research council and the traditional medicine department of the Barij Essence Pharmaceutical Company for financial support.

References

- [1] R.C. Srivastava, M.M. Husain, S.K. Hasan, M. Athar, *Cancer Lett.* **153**, 1 (2000).
- [2] R.G. Andrade, L.T. Dalvi, J.M. Silva, G.K. Lopes, A. Alonso, M. Hermes-Lima, *Arch. Biochem. Biophys.* **437**, 1 (2005).
- [3] T. Yugarani, B.K. Tan, N.P. Das, *Planta Med.* **59**, 28 (1993)
- [4] K.C. Ong, H.E. Khoo, N.P. Das, *Experientia* **51**, 577 (1995)
- [5] G.D. Stoner, C.S. Mandal, E.M. Daniel, Y.H. Heur, *Proc. Am. Assoc. Cancer Res.* **32**, 472 (1991).
- [6] G. Achilli, G.P. Cellerino, P.H. Gamache, *J. Chromatogr.* **632**, 111 (1993).
- [7] H.J. Wan, Q.L. Zou, R. Yan, F.Q. Zhao, B.Z. Zeng, *Microchim. Acta.* **159**, 109 (2007).
- [8] E. Haslam, *Chemistry and Pharmacology of Natural Products. Plant Polyphenols. Vegetable Tannins Revisited*, Cambridge University Press, Cambridge, (1989).
- [9] M. Brune, L. Rossander, L. Hallberg, *Eur. J. Clin. Nutr.* **43**, 574 (1989).
- [10] P. Geisser, *Arzneimittelforschung.* **40**, 754 (1990).
- [11] I. Bala, V. Bhardwaj, S. Hariharan, M.N.V. Ravi Kumar, *J. Pharmaceut. Biomed.* **40**, 206 (2006).
- [12] T.C. Wilson, A.E. Hagerman, *J Agric Food Chem.* **38**, 1678 (1990).
- [13] Z. Behong, W. Zhenhua, L. Xiaojun, Z. Jie, H. Xianming, *Phytochem. Anal.* **19**, 86 (2008).
- [14] L.R. Junior, J.C.B. Fernandes, G.O. Neto, *J. Electroanal. Chem.* **481**, 34 (2000).
- [15] J. Kang, L. Zhuo, X. Lu, X. Wang, *J. Solid, State Electrochem.* **9**, 114 (2005).
- [16] L. Xu, N. He, J. Du, Y. Deng, *Electrochem. Commun.* **10**, 1657 (2008).
- [17] L. Xu, N. He, J. Du, Y. Deng, Z. Li, T. Wang, *Anal. Chim. Acta.* **634**, 49 (2009).
- [18] A.J. Bard, L.R. Faulkner, *Electrochemical Methods: Fundamentals and Applications*, 2nd ed., Wiley, New York, (2001).
- [19] C.G. Zoski, *Handbook of electrochemistry*, New Mexico State University, Elsevier, Las Cruces, New Mexico, USA, (2007).
- [20] G. Kaur, M. Athar, M.S. Alam, *Chem-Biol Interact.* **171**, 272 (2008).
- [21] A.F. Aguilera-Carbo, C. Augur, L.A. Prado-Barragan, C.N. Aguilar, E. Favela-Torres, *Chem. pap.* **62**, 440 (2008).